Analysis of heat transfer in unlooped and looped pulsating heat pipes

M.B. Shafii and A. Faghri
Department of Mechanical Engineering, University of Connecticut, Storrs, USA
Yuwen Zhang
Department of Mechnical Engineering, New Mexico State University, Las Cruces, USA

Received September 2001
Accepted March 2002

Keywords *Heat transfer, Condensation, Tubing*

Abstract *An advanced heat transfer model for both unlooped and looped Pulsating Heat Pipes (PHPs) with multiple liquid slugs and vapor plugs has been developed. The thin film evaporation and condensation models have been incorporated with the model to predict the behavior of vapor plugs and liquid slugs in the PHP. The results show that heat transfer in both looped and unlooped PHPs is due mainly to the exchange of sensible heat. Higher surface tension results in a slight increase in the total heat transfer. The diameter, heating wall temperature, and charging ratio have significant effects on the performance of the PHP. Total heat transfer significantly decreased with a decrease in the heating wall temperature. Increasing the diameter of the tube resulted in higher total heat transfer. The results also showed that the PHP could not operate for higher charge ratios.*

Nomenclature

A = tube cross sectional area, m^2
B = number of bends
C_l = friction coefficient
c_p = specific heat (constant pressure), J/kg K
c_v = specific heat (constant volume), J/kg K
d = diameter, m
g = gravitational acceleration, m^2/s
h = enthalpy, J/kg
h_{fg} = latent heat, J/kg
k = thermal conductivity, W/mK
K = curvature, 1/m
L = length, m
L_h = length of heating section, m
L_c = length of cooling section, m
m = mass, kg
$\dot{m}$ = mass flow rate, kg/s
N = total number of vapor plugs
n = number of parallel tubes
N_p = total number of plugs
P = pressure, Pa
Pr = Prandtl number
Q = heat transfer rate (W)
R = gas constant, J/kg K
Re = Reynolds number
s = coordinate in meniscus, m
t = time, s
u = internal energy, J/Kg
T = temperature, K
V_v = volume of vapor, m^3
v_l = velocity of liquid plug, m/s
X = distance, m

Funding for this work was provided by NASA grant NAG3-1870 and NSF grant CTS 9706706.

International Journal of Numerical Methods for Heat & Fluid Flow, Vol. 12 No. 5, 2002, pp. 585-609.

DOI 10.1108/09615530210434304

Greek

α = charge ratio or contact angle
α_1 = thermal diffusivity of liquid, m/s^2
μ = dynamic viscosity, kg/ms
ρ = density, kg/m^3
σ = surface tension, N/m
σ_0 = Normal value of surface tension, N/m
τ = shear stress, N/m^2

Subscripts

in = inlet
l*i* = *i*th liquid plug
le = left end
out = outlet
re = right end
v*i* = *i*th vapor plug

1. Introduction

Thermal management has been considered as one of the most critical technologies in electronic product development. The heat pipe is one of the effective heat transfer devices being used in industry to remove heat from heat sources. With continued down- sizing of computers and processors, extensive studies have been done in order to provide better-designed and higher-efficiency heat pipes (Faghri, 1995; 1999). The Pulsating Heat Pipe (PHP), is one of the very promising heat transfer devices, that has been recently investigated by many engineers and scientists around the world. There is no wick structure used in PHPs, so its simple and cheap structure has made the PHP very attractive compared with conventional heat pipes. The PHP is made from a long continuous, capillary tube bent into turns. There are two types of PHPs: the looped pulsating heat pipe and the unlooped pulsating heat pipe. In the looped PHP the two ends of the tube are connected to one another and the working fluid is able to circulate. Unlike looped PHPs, the two ends are sealed in the unlooped PHP. The diameter of a PHP should be small enough (0.1–5 mm) so that vapor plugs can be formed by capillary action. Experiments show that PHPs can operate successfully for all operation modes, including both horizontal and vertical. When a capillary tube is partially filled, its working fluid will break up into a number of vapor plugs and liquid slugs along the tube due to the effect of surface tension, which is very significant in the small diameter tubes. The heat input, which is the driving force, increases the pressure of vapor plugs in the evaporator, and the heat output decreases the pressure of vapor plugs in the condenser. This pressure difference between condenser and evaporator causes the oscillation of vapor plugs and liquid slugs in the PHP. Many researchers have carried out both experimental and analytical studies. Due to the complicated behavior of working fluid in PHPs, the experimental investigations focus mainly on visualization of flow pattern and measurement of temperature and effective thermal conductivity.

Lee *et al.* (1999) reported that the most active oscillations were observed at charging ratios of 40–60 per cent for the PHP in vertical mode. It was also mentioned that nucleate boiling in the evaporator section caused oscillation of the working fluid. Kiseev and Zolkin (1999) investigated the effects of acceleration and vibration on the performance of PHPs. The experimental results showed that PHPs can operate successfully in various acceleration

fields. Hosoda *et al.* (1999) performed experiments on the propagation phenomena of vapor plugs in a meandering closed loop heat transport device (MCL-HTD). A simple flow pattern was observed for high charging ratios and low temperature differences. In their experiments, two vapor plugs existed separately in adjacent turns. Their results showed that while one of the adjacent plugs is growing, the other one shrinks. When the shrinking plug disappears, a new vapor plug appears in the turn adjacent to that containing the expanding vapor plug.

Using a Lagrangian approach, Wong *et al.* (1999) proposed a simple theoretical model of the PHP. The capillary heat pipe is modeled under adiabatic conditions and a sudden pressure pulse is applied to a vapor plug to simulate local heat input. The propagation of the pressure disturbance was investigated and it was concluded that the length of the vapor plugs and liquid slugs affects the propagation of the pressure wave inside a PHP.

Zhang and Faghri (2002) analyzed heat transfer in an open-ended PHP. Evaporation and condensation in the evaporator and condenser sections of an open-ended PHP were modeled by analyzing thin film evaporation and condensation. The results showed that the heat transfer in a PHP is due mainly to the exchange of sensible heat. Shafii *et al.* (2001) proposed analytical models for both unlooped and looped PHPs. In their model, heat transfer coefficients were assumed to be constant in the heating and cooling sections. Their results showed that the heat rejected from the system (unlooped and looped) significantly decreased with the decreasing wall temperature of the heating section and the total heat transferred by the PHP was due mainly to sensible heat. They also showed that the total number of vapor plugs was equal to the total number of bends passing through the heating section regardless the umber of vapor plugs initially in the PHP. In the present study, the effect of thin film evaporation and condensation will be implemented into the model proposed by Shafii *et al.* (2001) for both unlooped and looped PHPs, and the effects of various geometric and physical parameters on the performance of PHPs will be investigated.

2. Theoretical model

Figures 1(a) and 1(b) show a physical model of the unlooped and looped PHPs. The bends are not considered in the present study and it is assumed that the PHP is a straight tube (Figure 1(c)). There are three vapor plugs and two liquid slugs in the PHP (Shafii *et al.*, 2001). The pressure and temperature of all vapor plugs are initially equal. A control volume of a liquid slug bounded with two vapor plugs is shown in Figure 2. When a liquid slug moves due to expansion of the adjacent vapor plug in the heating section, it leaves a thin liquid film behind on the wall. Evaporation will take place from this thin film (Zhang and Faghri, 2001). Heat transfer coefficients in the heating and cooling sections will

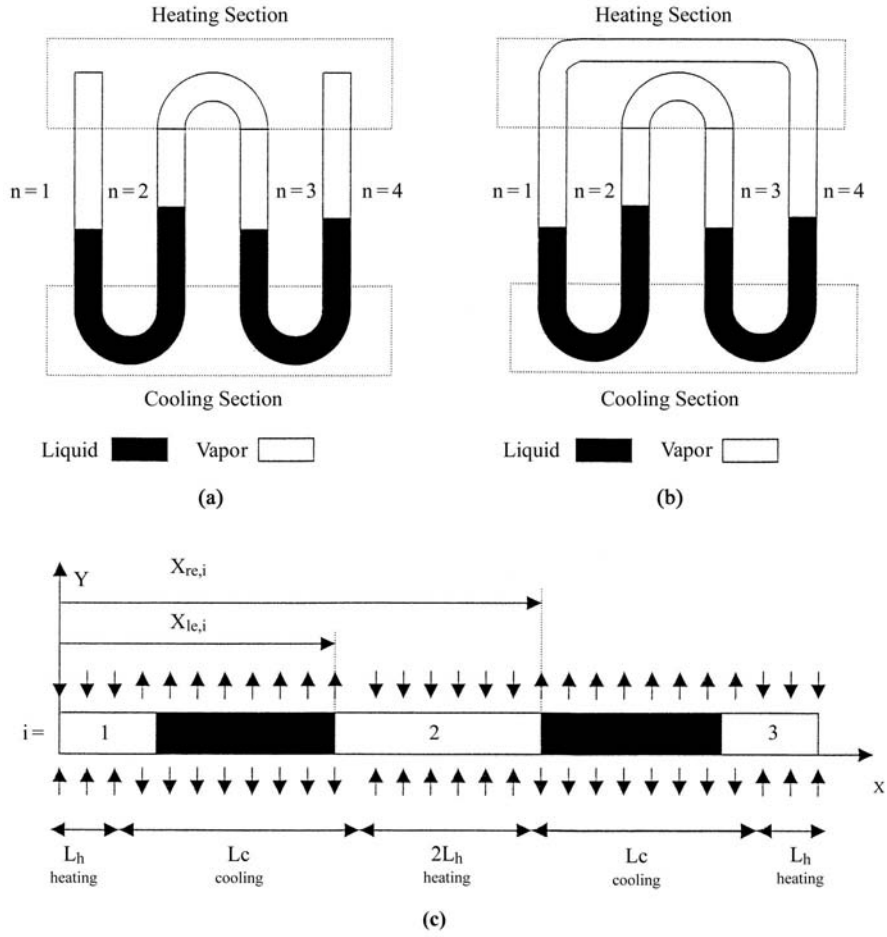

Figure 1.
Oscillating heat pipes: (a) unlooped PHP; (b) looped PHP; (c) dimensional variables of the model

be obtained by analyzing this existing thin film in the evaporator and condenser.

The following assumptions are made in order to model heat transfer and pulsating flow in the heat pipe:

(1) The liquid is incompressible and the vapor plugs are assumed to behave as ideal gases.

(2) Heat transport in the thin film is due only to the conduction in the radial direction.

(3) Shear stress at the liquid-vapor interface is negligible.

(4) Inertia terms can be neglected for viscous flow in the liquid films since the Reynolds number is low.

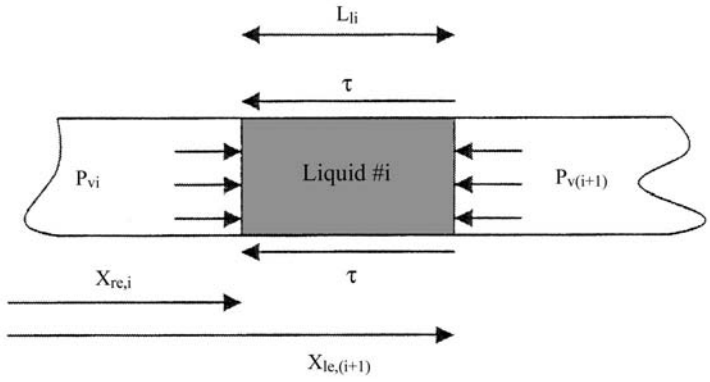

Figure 2.
Control volume of *i*th liquid plug

3. Governing equations

3.1 Liquid slugs and vapor plugs

The momentum equation for *i*th liquid slug is

$$\frac{\mathrm{d}m_{li}v_{li}}{\mathrm{d}t} = (P_{vi} - P_{v(i+1)})A - \pi \mathrm{d}L_{li}\tau \tag{1}$$

The effect of gravity is not taken into account since it is negligible (Shafii *et al.*, 2001). The shear stress acting between *i*th liquid slug and the tube and can be determined from

$$\tau = \tfrac{1}{2}C_{li}\rho_l v_{li}^2 \tag{2}$$

where the friction coefficient can be determined by

$$C_{li} = \begin{cases} \dfrac{16}{Re_{li}} & Re \le 1180 \\ 0.078Re_{li}^{-0.2} & Re > 1180 \end{cases} \tag{3}$$

The continuity equation for the *i*th vapor plug is

$$\frac{\mathrm{d}m_{vi}}{\mathrm{d}t} = \dot{m}_{\mathrm{in},vi} - \dot{m}_{\mathrm{out},vi} \tag{4}$$

where $\dot{m}_{\mathrm{in},vi}$ is the rate of mass transferred into the vapor plug due to evaporation, and $\dot{m}_{\mathrm{out},vi}$ is the rate of mass transferred from the vapor plug due to condensation of the *i*th vapor plug and can be calculated by the following equations:

$$\dot{m}_{\mathrm{in},vi} = Q_{\mathrm{evp},vi}/h_{\mathrm{fg}} \tag{5a}$$

$$\dot{m}_{\mathrm{out},vi} = Q_{\mathrm{cond},vi}/h_{\mathrm{fg}} \tag{5b}$$

where Q_{evp} and Q_{cond} represent heat transfer resulting from evaporation and condensation. The energy equation for a vapor plug is

$$m_{vi}c_v \frac{dT_{vi}}{dt} = (\dot{m}_{in,vi} - \dot{m}_{out,vi})RT_{vi} - P_{vi}A\frac{dX_{vi}}{dt} \tag{6}$$

The pressure of the ith vapor plug, P_{vi} is calculated by using the ideal gas law

$$P_{vi}V_{vi} = m_{vi}RT_{vi} \tag{7}$$

3.2 Evaporation

The physical model of thin film evaporation in the evaporator section is shown in Figure 3(a). The liquid film thickness in the evaporator section satisfies (Zhang and Faghri, 2002)

$$\frac{d}{dx}(\sigma K - p_d) = \frac{3\mu_l}{2\pi R\rho_l \delta^3}\left(\dot{m}_{l,in} - \frac{Q}{h'_{fg}}\right) \tag{8}$$

where K is the curvature of the liquid film and pd is the disjoining pressure. The revised latent heat of evaporation is defined as

$$h'_{fg} = h_{fg} + 0.68c_{PL}(T_h - T_{vi}) \tag{9}$$

and the rate of heat transfer is

$$Q = 2\pi R\int_0^{L_1} \frac{k_L(T_h - T_{vi})}{\delta} ds \tag{10}$$

The boundary conditions in the heating section (Figure 3(a)) are

$$\frac{d\delta}{dx} = 0, \quad \frac{d^2\delta}{dx^2} = \frac{1}{R - \delta_{tr}} \qquad x = 0 \tag{11a}$$

$$\delta = \delta_0, \quad \frac{d\delta}{dx} = \tan\alpha, \qquad x = L_1 \tag{11b}$$

δ_{tr} is the liquid film thickness at $x = 0$ and is yet unknown. δ_0 is the nonevaporating film thickness calculated by Khrustalev and Faghri (1995).

The film thickness δ can be found as a function of x by assuming a polynomial function for δ and using the above boundary conditions. Substituting this film thickness function into equation (8) yields

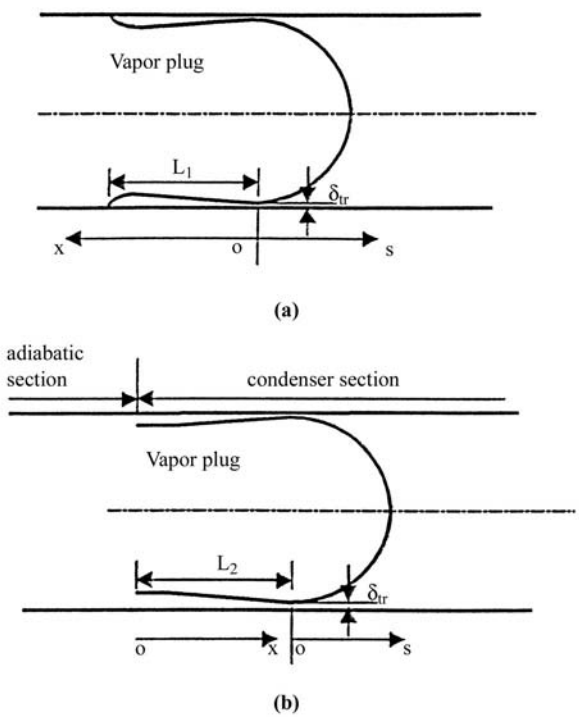

Figure 3.
The physical model of film thickness in heating and cooling sections

$$\rho_l R_g T_{vi} b \ln\left(\frac{\delta_{tr}}{\delta_0}\right) + \sigma \frac{(\delta_0 - \delta_{tr})}{(R - \delta_0)(R - \delta_{tr})} - \frac{6L_1 \tan\alpha - 12(\delta_0\, \delta_{tr})}{L_1^2}$$

$$= \frac{3\mu_L}{2\pi R \rho_l} \int_0^{L_1} \frac{1}{\delta^3} \left(\dot{m}_{l,in} - \frac{Q}{h'_{fg}}\right) dx \tag{12}$$

The mass flow rate of liquid at $x = 0$ is determined by an overall energy balance

$$\dot{m}_{l,in} = \frac{Q}{h_{fg}} \quad \text{at } x = L_1 \tag{13}$$

From equations (12) and (13), the liquid film thickness at the transition (δ_{tr}) can be found using an iteration method. The total heat transfer amount for the entire thin film is then

$$Q_{e1} = 2\pi R k_l (T_h - T_{vi}) \int_0^{L_1} \frac{1}{\delta} dx \tag{14}$$

Evaporation at the meniscus must be calculated. The thickness beyond the transition point is calculated by

$$\delta_m = R - \sqrt{(R - \delta_{\mathrm{tr}})^2 + s^2} \tag{15}$$

The heat transfer in the meniscus region is then

$$Q_{e2} = 2\pi R k_l (T_h - T_{\mathrm{v}i}) \int_0^{R-\delta_{\mathrm{tr}}} \frac{1}{\delta_m} \mathrm{d}s \tag{16}$$

and the total evaporative heat transfer for the evaporator section is

$$Q_{\mathrm{evp}} = Q_{e1} + Q_{e2}. \tag{17}$$

3.3 Condensation

The physical model of film condensation in the condenser section is shown in Figure 3(b). The liquid film thickness in the condenser section satisfies (Zhang and Faghri, 2002)

$$\frac{\sigma h_{\mathrm{fg}} \rho_l}{3\mu_l} \left[\delta^3 \left(\frac{\mathrm{d}^3\delta}{\mathrm{d}x^3} + \frac{1}{(R-\delta)^2} \frac{\mathrm{d}\delta}{\mathrm{d}x} \right) \right] = k_l (T_{\mathrm{v}i} - T_c) \int_0^s \frac{1}{\delta} \mathrm{d}s \tag{18}$$

The boundary conditions for cooling sections (Figure 3(b)) can be written as

$$\frac{\mathrm{d}\delta}{\mathrm{d}x} = 0, \quad \frac{\mathrm{d}^2\delta}{\mathrm{d}x^2} = 0 \qquad x = 0 \tag{19a}$$

$$\frac{\mathrm{d}\delta}{\mathrm{d}x} = 0, \quad \frac{\mathrm{d}^2\delta}{\mathrm{d}x^2} = \frac{1}{R - \delta_{\mathrm{tr}}} \qquad x = L_2 \tag{19b}$$

The film thickness, δ, can be found as a function of x by assuming a polynomial function for δ and using the above boundary conditions. Substituting this function into equation (18) at $x = L_2$ yields

$$\frac{\sigma h_{\mathrm{fg}} \rho_l}{3\mu_l} \left[\frac{\delta_{\mathrm{tr}}^3}{R - \delta_{\mathrm{tr}}} \right] = k_l (T_{\mathrm{v}i} - T_c) \int_0^{L_2} \frac{1}{\delta} \mathrm{d}x \tag{20}$$

From equation (20), the liquid film thickness at the transition point, δ_{tr}, can be found using an iteration method. The total heat transfer amount for the entire thin film is then

$$Q_{c1} = 2\pi R k_l (T_{vi} - T_c) \int_0^{L_1} \frac{1}{\delta} \mathrm{d}x \tag{21}$$

Condensation at the meniscus must be calculated. The thickness beyond the blocking point is calculated by

$$\delta_m = R - \sqrt{(R - \delta_{tr})^2 + s^2} \tag{22}$$

The heat transfer in the meniscus region is then

$$Q_{c2} = 2\pi R k_l (T_{vi} - T_c) \int_0^{R-\delta_{tr}} \frac{1}{\delta_m} \mathrm{d}s \tag{23}$$

and the total condensation heat transfer amount for the condenser is

$$Q_{cond} = Q_{c1} + Q_{c2}. \tag{24}$$

3.4 Sensible heat transfer

Heat transfer in a PHP is defined as the total heat transferred from the heating sections to the cooling sections. Part of the heat transfer is due to evaporation and condensation of the working fluid. Another part is due to heat transfer between the tube wall and liquid slugs in the form of single-phase heat transfer. Evaporation and condensation heat transfer for each vapor plug can be calculated by

$$Q_{in,vi} = \dot{m}_{evp,vi} h_{fg} \tag{25a}$$

$$Q_{out,vi} = \dot{m}_{cond,vi} h_{fg} \tag{25b}$$

The single-phase heat transfer between the tube wall and liquid slugs is obtained by solving the energy equation for a liquid slug

$$\frac{1}{\alpha_l} \frac{\mathrm{d}T_{li}}{\mathrm{d}t} = \frac{\mathrm{d}^2 T_{li}}{\mathrm{d}x^2} - \frac{h_{lsen} \pi D}{k_l A} (T_{li} - T_w) \tag{26}$$

with the following boundary conditions

$$T_{li} = T_{vi} \qquad x = x_{re,i} \tag{27a}$$

$$T_{li} = T_{v(i+1)} \qquad x = x_{le,(i+1)} \tag{27b}$$

Since the Reynolds number of the liquid slug varies in a wide range that covers laminar, transition, and turbulent flow, the heat transfer coefficient h_{lsen} of the liquid slug varies, and it is calculated by using appropriate empirical correlations (Shafii *et al.*, 2001).

The heat transferred into and out of the liquid slug are

$$Q_{\text{in},li} = \int_{X_{\text{re},i}}^{X_{\text{le},(i+1)}} \pi D h_x (T_{li,x} - T_w) \mathrm{d}x \qquad T_{li} \geq T_w \tag{28a}$$

$$Q_{\text{out},li} = \int_{X_{\text{re},i}}^{X_{\text{le},(i+1)}} \pi D h_x (T_w - T_{li,x}) \mathrm{d}x \qquad T_{li} \leq T_w \tag{28b}$$

where $T_{li,x}$ represents the temperature of the ith liquid plug at x location. The total heat transferred into and out of the PHP can be calculated by

$$Q_{\text{total,in}} = \sum\nolimits_{i=1}^{N} Q_{\text{evp,iv}} + \sum_{i=1}^{N-1} Q_{\text{in},li} \tag{29a}$$

$$Q_{\text{total,out}} = \sum_{i=1}^{N} Q_{\text{cond,iv}} + \sum_{i=1}^{N-1} Q_{\text{out},li}. \tag{29b}$$

4. Numerical procedure

The new values at time $t + \mathrm{d}t$ can be found explicitly from the old values at time t. The displacement and the end positions of the vapor plugs at each time step can be found by using the liquid slug velocity obtained from equation (1). The detailed numerical procedure can be found in Shafii *et al.* (2001). In order to obtain the time step independent solution of for both unlooped and looped PHPs, the time step was varied systematically. It was found that varying the time step from 5×10^{-6} s to 10^{-7} s results in less than 0.2 per cent variation in the locations of the liquid slugs, and the time step used in the numerical solution is 5×10^{-6} s.

In order to compute sensible heat transfer for the PHP, the temperature distribution in the liquid slug is obtained by solving equation (26) using an implicit scheme (Patankar, 1980). A nonuniform grid was chosen in order to solve the energy equation for the liquid slugs. The total number of nodes chosen is 360, of which 140 belong to each end (3 cm) and 80 grids correlate with the middle of each liquid slug. The effect of change in the increased number of nodes on the results was tested and negligible dependency between them was observed. Decreasing the time step to 10^{-4} s results in 0.2 per cent variation in temperature distribution along the liquid slugs. The time step used in the numerical solution is 10^{-3} s.

5. Results and discussion

5.1 Unlooped PHP

The parameters used are listed in Table I. The lengths of liquid slugs are equal and can be found based on the charge ratio of the system. The parametric study

Working Fluid	Water
Initial pressure of vapor plugs	$P_{vi} = 47390\,\text{Pa}$
Initial temperature of vapor plugs	$T_{vi} = 80℃$
Percentage filled	$\alpha = 68.4\%$
Total length	$L = 1.14\,\text{m}$
Total number of plugs	$N_p = 5$
Number of bends	$B = 3$
Length of each vapor plug	$L_{v1} = L_{v2} = 0.09\,\text{m}$, $L_{v2} = 0.18\,\text{m}$
Wall temperature in cooling section	$T_c = 20℃$
Wall temperature in heating section	$T_h = 120℃$
Diameter	$d = 0.0015\,\text{m}$
Length of heating section	$L_h = 0.1\,\text{m}$
Length of cooling section	$L_c = 0.37\,\text{m}$
Normal value of surface tension	$\sigma_0 = [75.83 - 0.1477(T_v - 273.15] \times 10^{-3}\,\text{N/m}$

Table I.
Initial values of PHP

of PHPs in the following section will be performed for three vapor plugs in the heating sections. Figure 4 shows the variations of pressure, temperature and positions of the two ends of the first vapor plug with respect to time using parameters listed in Table I. It can be seen that since the right end is initially in

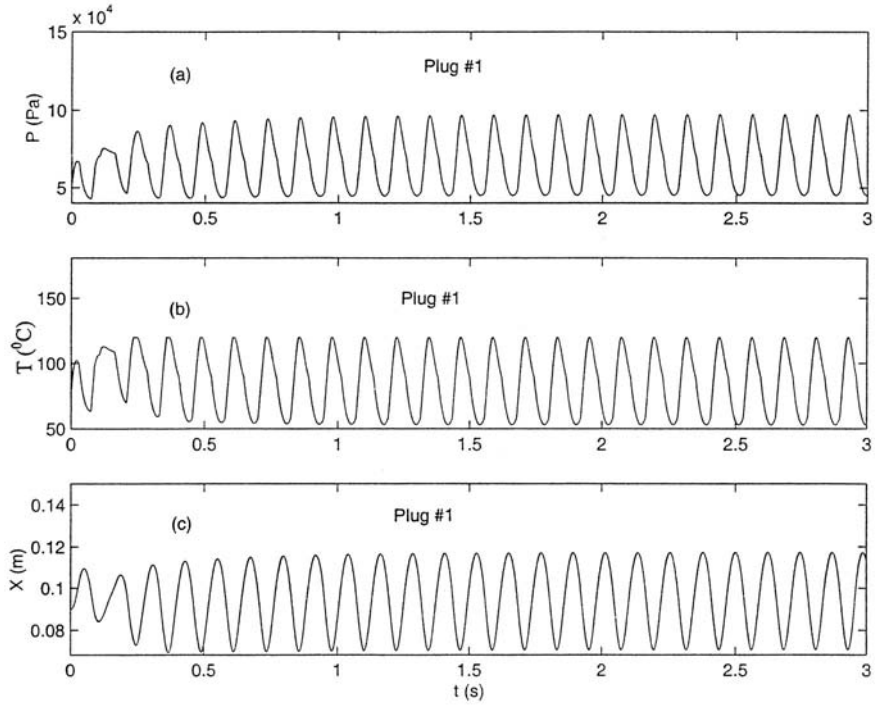

Figure 4.
Variation of pressure, temperature and the end positions of the first plug with time and comparison with the previous model

the heating section, evaporation takes place and both temperature and pressure rise to certain values. The higher pressure in the first vapor plug causes the first liquid slug to move toward the cooling section. Once the right end reaches the cooling section, condensation takes place and both temperature and pressure drop. When the pressure is low enough, the adjacent liquid slug starts moving back to the heating section. As it moves back, the temperature of the first vapor plug increases due the compression; however, condensation is still taking place. When the right end moves into the heating section, evaporation takes place. The pressure and temperature of the vapor plug keep increasing until the pressure in the vapor plug is high enough to push the adjacent liquid slug toward the cooling section. This phenomenon repeats itself and periodic oscillation is established after 1 s. The temperature of the first vapor plug has its maximum value, which is the heating wall temperature, when it is completely compressed in the heating section. At this point, pressure also reaches its maximum, at 9×10^4 Pa. Figure 4(c) shows the position of the two ends of the first vapor plug. Since the first vapor plug is located at the end of the PHP, the left end is always located at $x = 0$ m. The right end oscillates between $x = 0.07$ m and $x = 0.12$ m.

Figure 5 shows the variations of pressure, temperature and positions of the two ends of the second vapor plug. Since the two ends are free to move into the heating and cooling sections, the amplitude of the oscillation is low. Most of the time when one end is in the heating section the other end would be in the cooling section, and this causes small variation in temperature of the vapor plug (Figure 5(b)). Consequently, the variation in the pressure of the plug is also low (Figure 5(b)). Figure 5(c) shows the positions of the two ends of this vapor plug. The solid and dashed lines represent the location of the right and left ends. The distance between these two lines indicates the length of the vapor plug. The two ends always move in the same direction, and when one moves into the heating section the other one moves into the cooling section. Figure 6 represents pressure, temperature and position variations of the two ends of the third vapor plug with time. The oscillating trends of pressure, temperature and position of the ends are the same as those of the first vapor plug and the phase difference is 180°.

The rate of evaporative and condensation heat transfer of each individual vapor plug, when periodic oscillation is obtained, is shown in Figure 7. It can be seen from Figure 7(a) that when the right end of the first vapor plug moves into the heating section, the evaporative heat transfer suddenly jumps to its maximum value. Then it starts decreasing to its minimum value as the right end continues moving inside the heating section and compresses the first vapor plug. Meanwhile, the temperature of the vapor plug increases due to evaporation and compression. When the temperature of the vapor plug reaches the heating wall temperature, evaporation stops and there is no heat transferred into the vapor plug. As the vapor expands, its temperature drops

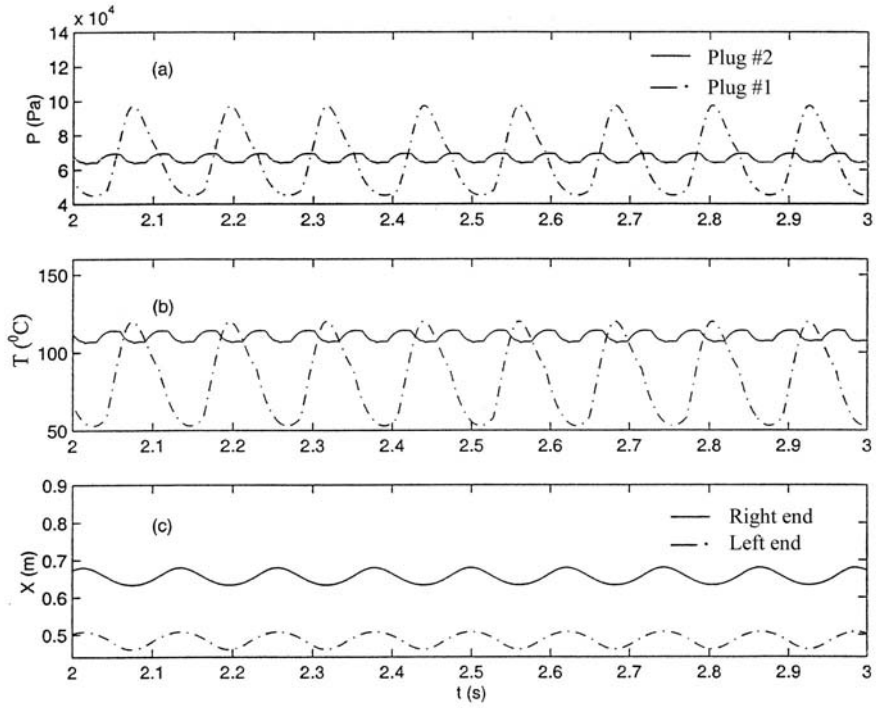

Figure 5.
Variation of pressure, temperature and the end positions of the second plug with time

and heat transfer increases until the right end moves into the cooling section where condensation occurs. Figure 7(b) shows the rate of evaporative and condensation heat transfer of the second vapor plug. The evaporative heat transfer jumps suddenly when one of the ends enters or exits the heating section. It can be seen that when both ends are in the heating section, the condensation heat transfer is zero and the temperature of the vapor plug increases causing the evaporative heat transfer to decrease. Figure 7(c) reflects the second vapor plug behaves exactly as the first vapor plug, with a 180° phase difference.

The variation of the sensible heat transferred into and out of the liquid slugs is shown in Figure 8. Since the charge ratio is high, a part of the liquid slugs always remains in the heating section, and there is always sensible heat transferred into the slugs. The sudden changes in the sensible heat are due to the change from laminar flow to transition flow. The total heat transferred into the PHP for this case is 31.93 W. The total sensible heat transferred is 30.49 W and this means that 95.5 per cent of the heat transferred into the system is due to the sensible heat.

The effect of surface tension on the performance of the PHP is shown in Figure 9. The frequency of the oscillation is almost unchanged; however, the

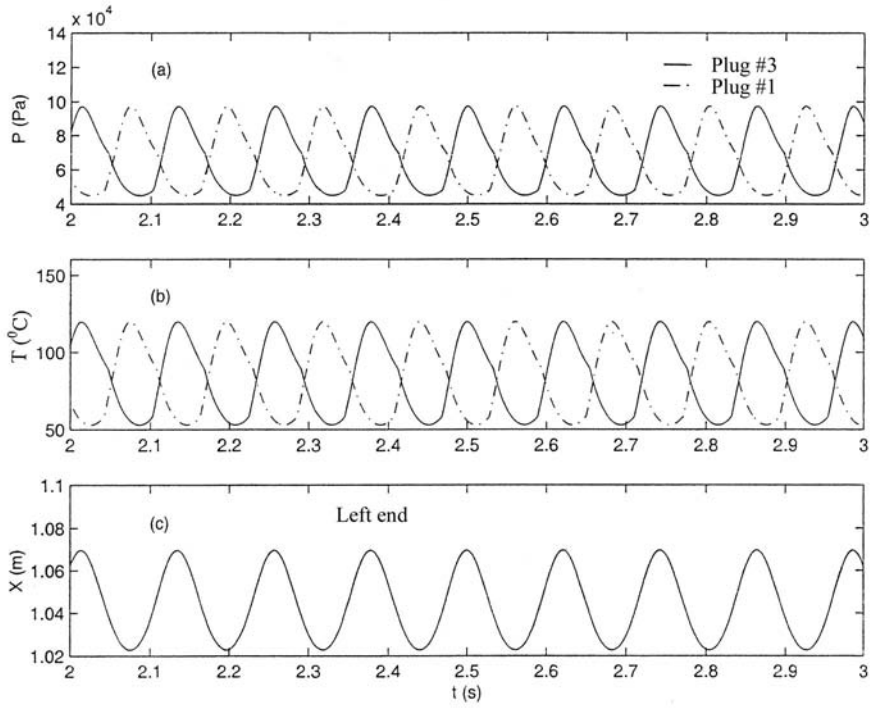

Figure 6.
Variation of pressure, temperature and the end positions of the third plug with time

amplitude increases for the case with higher surface tension. Since the first vapor plug moves farther into the cooling section, the minimum temperature of the first vapor plug is lower (Figure 9(b)), and the evaporative heat transfer is higher (shown in Figure 10). The total evaporative heat transfer is 1.7 W. This is true since higher surface tension results in a thinner liquid film (Zhang *et al.*, 2001). The velocity variation with time for each individual liquid slug is shown in Figure 11. It can be observed that the velocities of liquid slugs are higher when the surface tension is greater, and this results in greater sensible heat transfer shown in Figure 12.

Figure 13 shows the effect of the heating wall temperature on the pressure, temperature and end positions of the first vapor plug. The parameters and thermal properties are similar to what is given in Table I, except that the wall temperature is reduced to 100°C. Decreasing the wall temperature reduces the magnitude of pressure and the location of the right end and it also slightly decreases the frequency of oscillation. It can be seen from Figure 13(b) that the average temperature of the first vapor plug decreases with decreasing wall temperature and the temperature difference between the wall and vapor plug decreases. This results in lower evaporative heat transfer, as shown in Figure 14. Figure 14 also indicates that the heat transferred into the vapor plugs

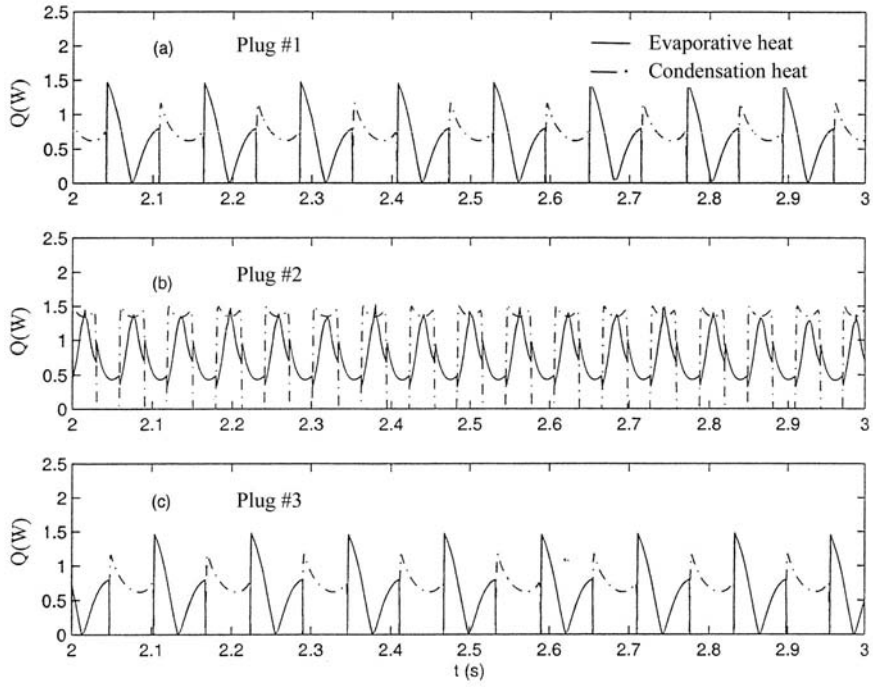

Figure 7.
The evaporative and condensation heat transfer rate

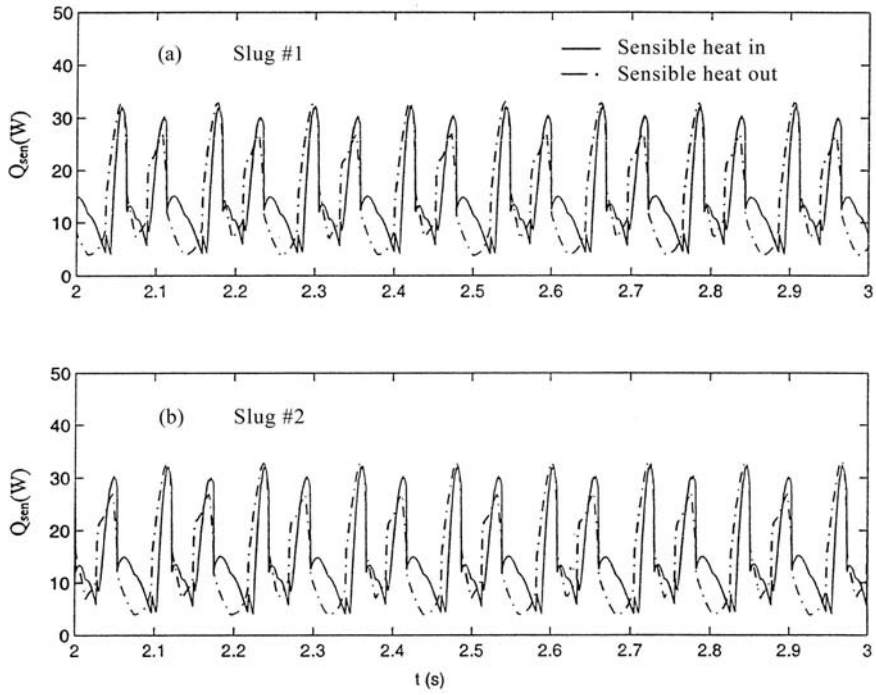

Figure 8.
Sensible heat transferred in and out of liquid slugs

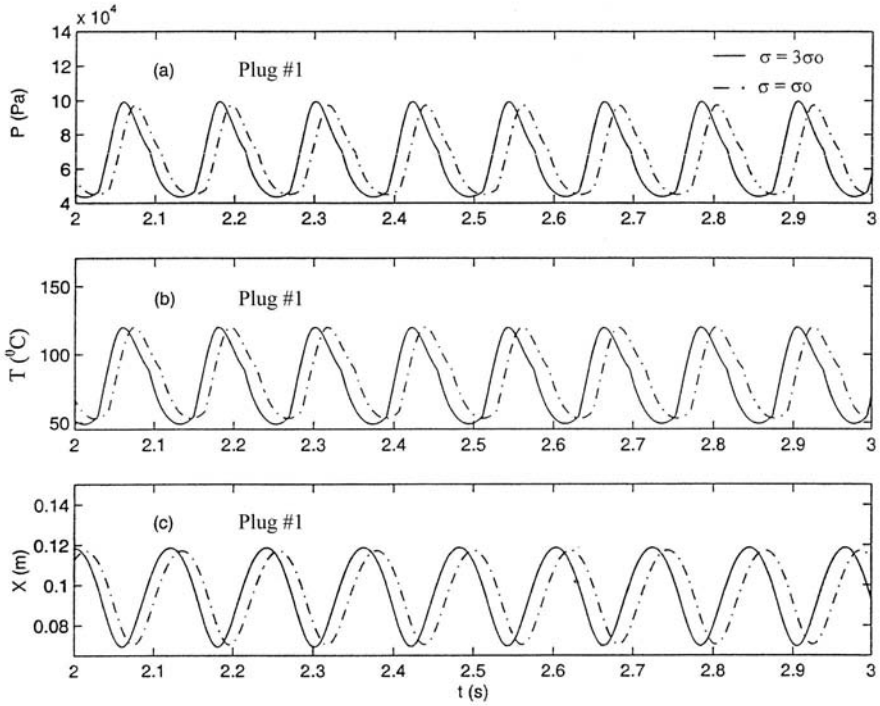

Figure 9.
Effect of surface tension on the performance of the first plug

decreases with decreasing temperature difference between the heating and cooling sections. The changes of the sensible heat transfer of each liquid slug with time are shown in the Figure 15. It can be seen that the sensible heat significantly decreases with a reduction in heating wall temperature. The sensible heat transfer depends on the velocity and the frequency of the oscillation of the liquid slugs. Since both decrease with a reduction in heating wall temperature, the total heat transfer significantly decreases. From calculated results, it can be concluded that a 16.6 per cent reduction in the temperature difference between the heating and cooling wall sections results in a nearly 30.54 per cent reduction in the total heat transferred into the PHP. The total heat transferred into the PHP for this case is 22.24 W in which the contribution of sensible heat is 95.18 per cent.

To investigate the effect of diameter on PHP performance, the diameter of the tube is increased to 3 mm. The other parameters and initial values are unchanged. Figure 16(a) shows the pressure variation with time for the first vapor plug. It can be observed that the frequency of oscillation is lower than that of the small diameter tube. From Figure 16(b) and (c) one can conclude that the average temperature of the first vapor plug is lower than that of the first

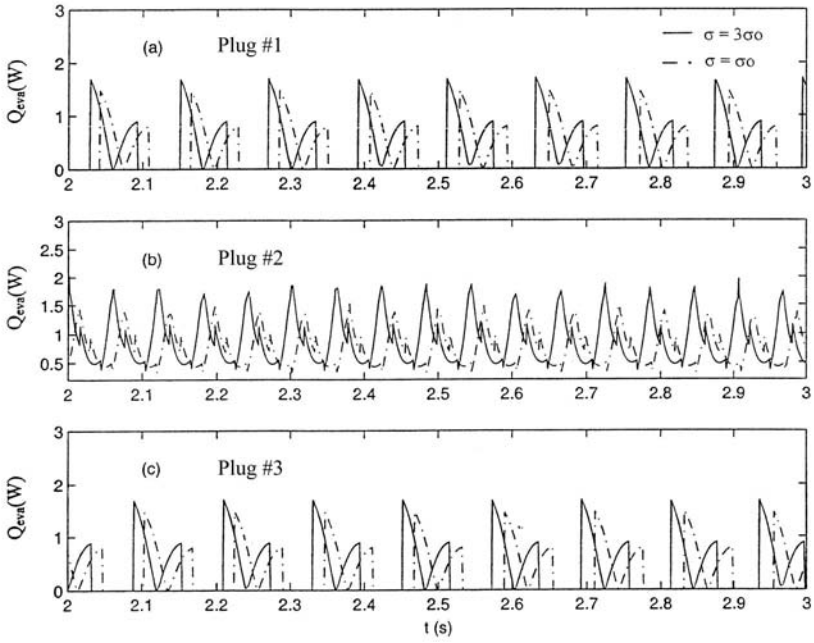

Figure 10.
Effect of surface tension on evaporative heat

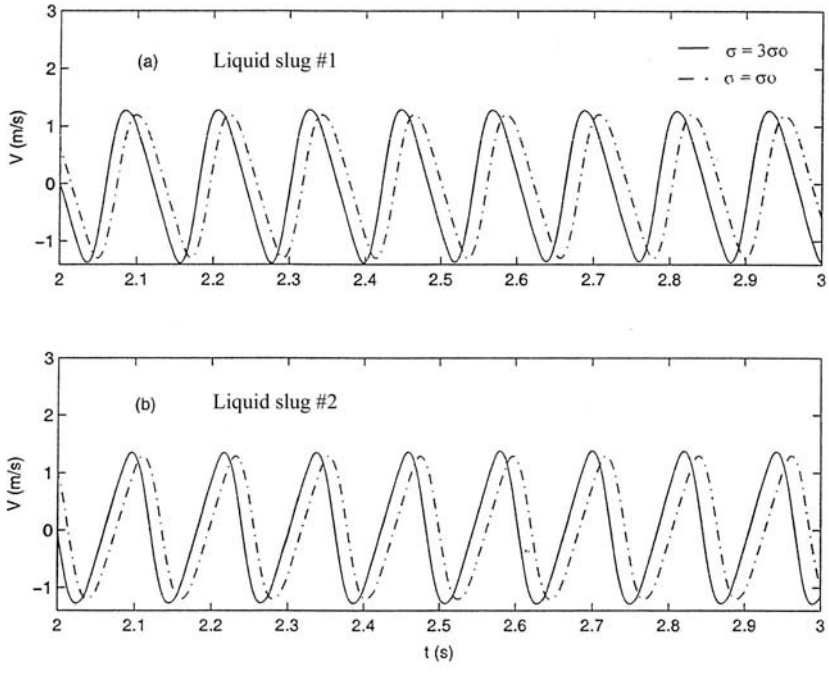

Figure 11.
Variation of the velocity of the liquid slugs with time

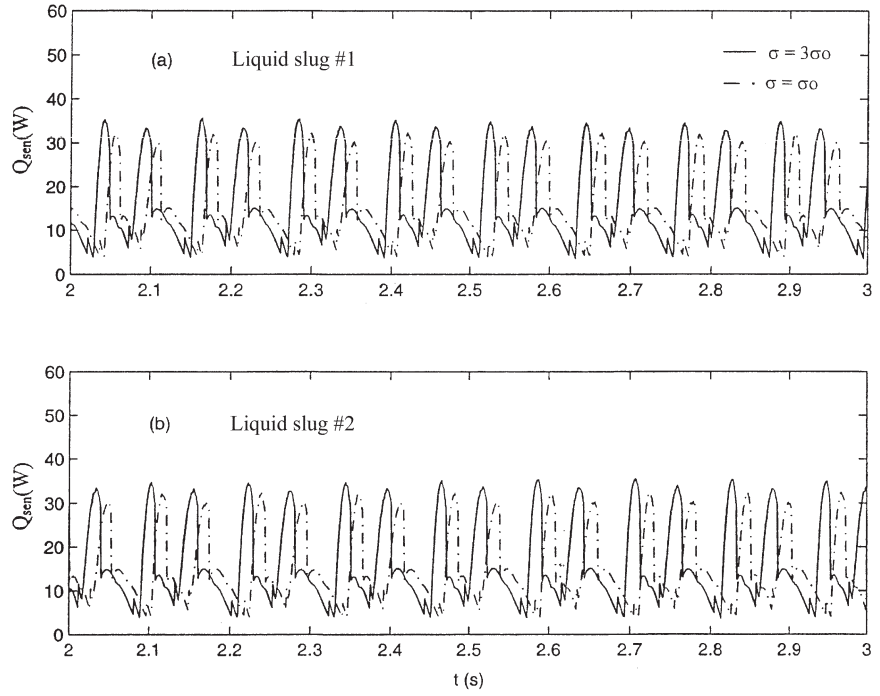

Figure 12.
Effect of the surface tension on sensible heat

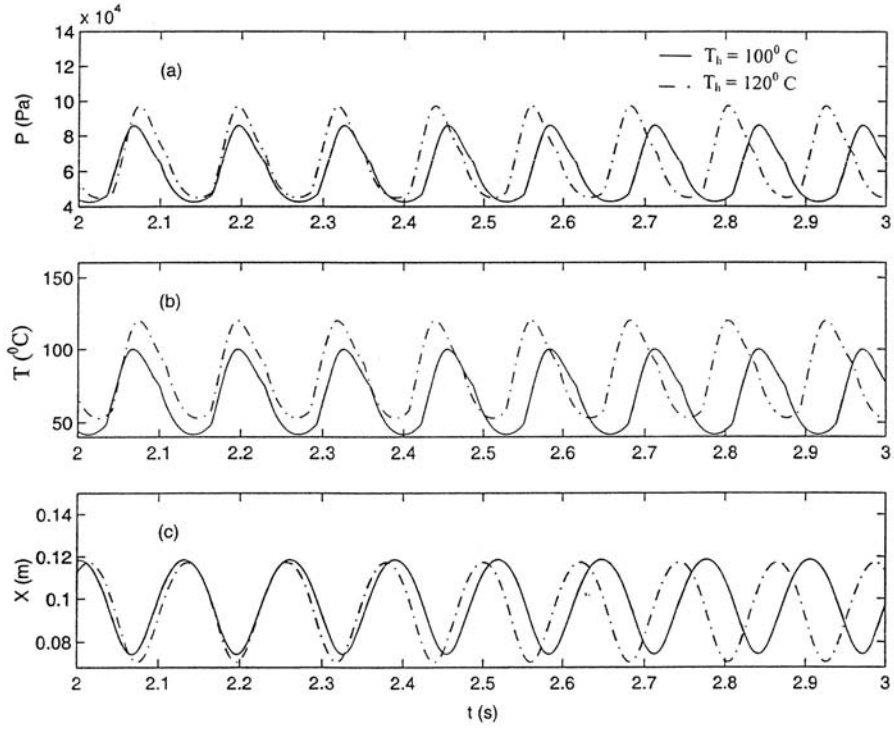

Figure 13.
Effect of the heating wall temperature on the performance of the first plug

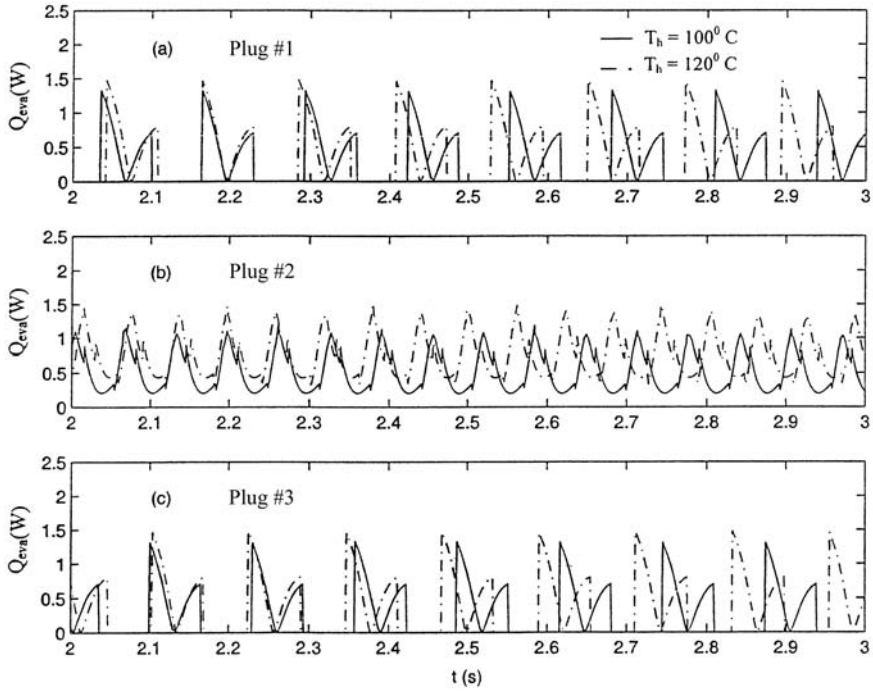

Figure 14.
Effect of the heating wall temperature on the evaporative heat

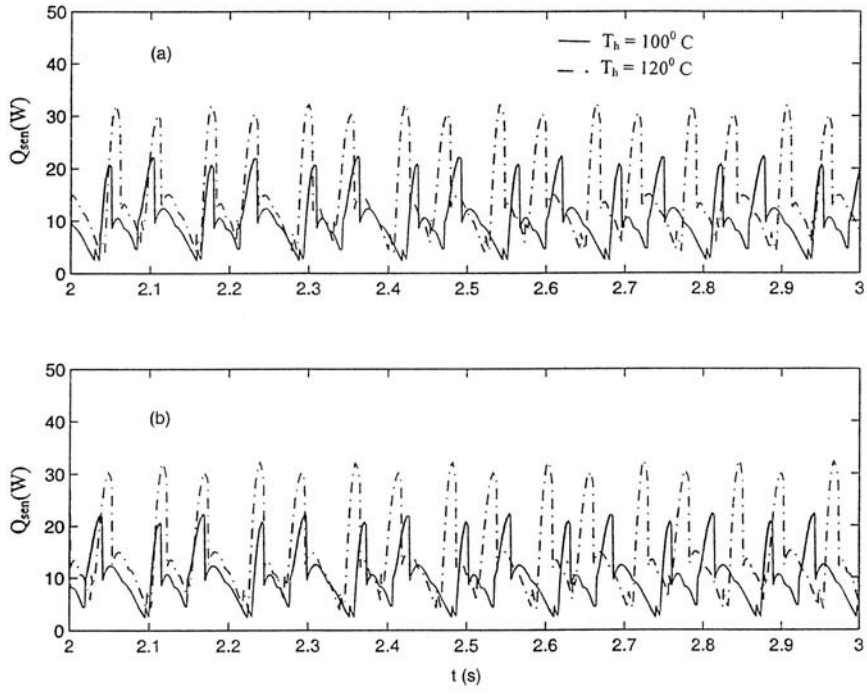

Figure 15.
Effect of the heating wall temperature on sensible heat

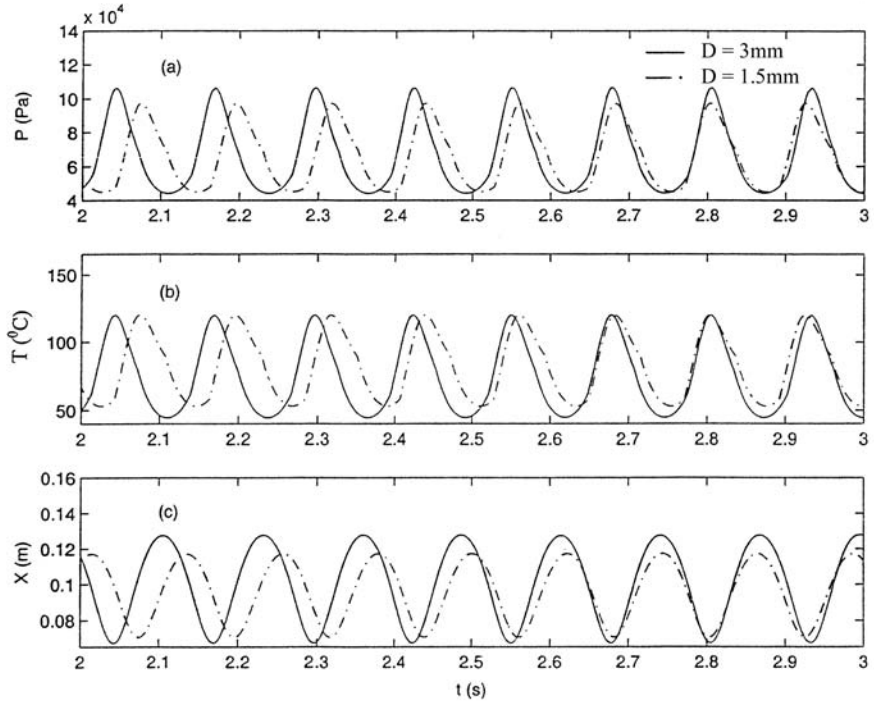

Figure 16.
Effect of diameter on the performance of the first plug

vapor plug in the small diameter tube by the time the right end moves in the heating section. Since the heating area and the temperature difference between the heating wall section and vapor plugs are greater than that of the small diameter tube, the evaporative heat is higher for all vapor plugs (Figure 17). The total heat transferred into the PHP for this case is 118.68 W, in which the contribution of the sensible heat is 97.06 per cent.

The effect of the charging ratio on PHP performance is shown in Figure 18. Here, the diameter of tube is 1.5 mm and the length of all liquid slugs is 0.51 m. The first and third vapor plugs have a length of 0.03 m and the second is twice as long as the other two. This yields a charge ratio of 89.4 per cent in the PHP. Figure 18 indicates that oscillation cannot occur when the charging ratio is high. When the charging ratio is high in the PHP, the liquid slugs are long, and a higher-pressure difference is needed to move the more massive liquid slugs. Since this pressure difference cannot be obtained, the temperature will rise to the heating wall temperature, and there will be no heat transferred into the plugs causing, thereby the PHP to not perform properly. This is consistent with experimental results presented by Gi *et al.* (1999). Their results showed that the heat transport rate decreased with increasing charge ratio for an unlooped PHP. The effects of different parameters, discussed above, on the heat transfer

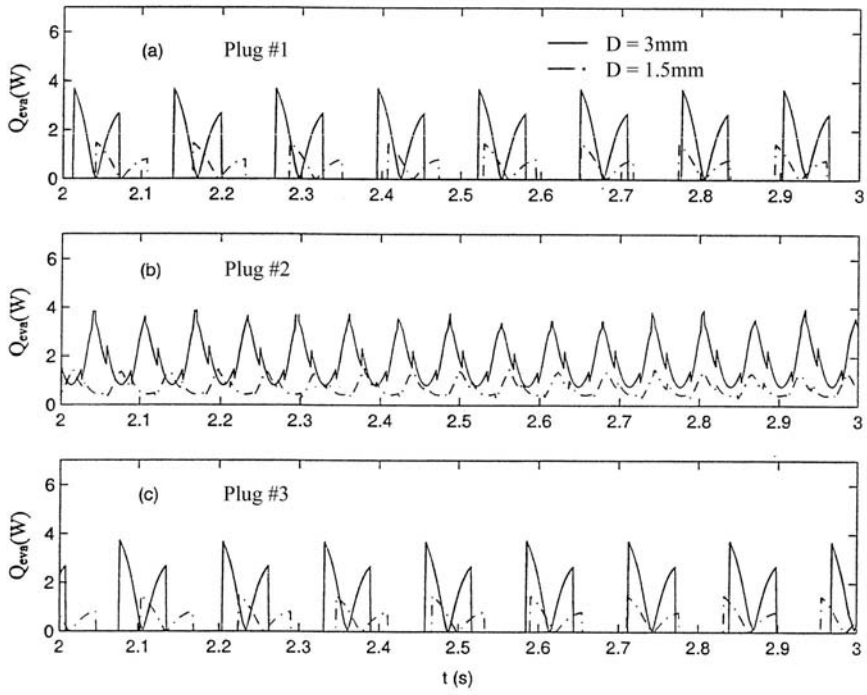

Figure 17.
Effect of diameter on the evaporative heat transfer rate

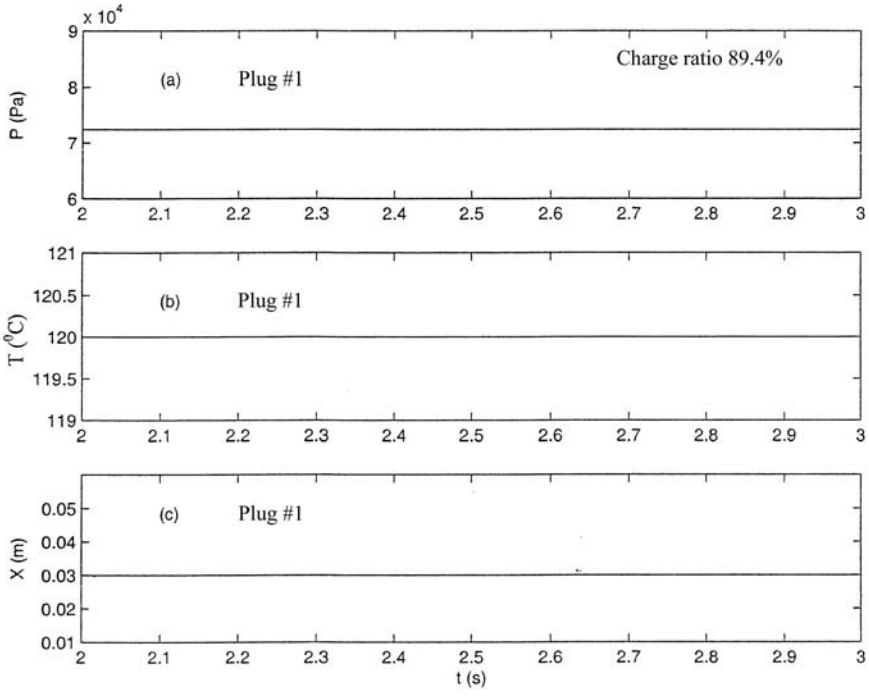

Figure 18.
Effect of the charge ratio on the performance of the first plug

performance of the unlooped PHP is listed in Table II. The results obtained based on the film theory are qualitatively consistent with the results obtained by Shafii *et al.* (2001).

5.2 Looped PHP

Miyazaki and Arikawa (1999) performed visualization experiments on a looped PHP and observed that the vapor plugs existed only in the heating sections. The behavior of liquid slugs and vapor plugs in looped PHPs is also investigated. The parameters listed in Table I are used except that the total number of plugs is $N = 4$. Also, the lengths of the first and second vapor plugs are equal due to the fact that the first and the last vapor plugs are connected to make one plug. The charging ratio is also assumed to be 64.21 per cent. Figure 19 shows the variations of pressure, temperature and positions of the two ends of the first and the second vapor plug with respect to time. Periodic oscillation occurs after $t = 0.2$ s. Since the initial pressure of the first vapor plug is higher than for the second one, the amplitudes of the pressure oscillations of the first and second plugs are slightly different, but the phase difference is 180°. Figure 19(b) indicates that the average and peak temperatures of the first vapor plug are lower than those of the first plug. The variation of sensible and evaporative heats with time is shown in Figure 20. The system is symmetric, and the sensible heat inputs for liquid slugs are overlapped. The total average sensible heat obtained from this system is 27.7 W. The temperature of the second vapor plug reaches the heating wall temperature at some particular time and that yields no heat transferred into the plug (Figure 20(b)). The total average evaporative heat is 1.44 W and this means 95 per cent of the heat rejected from the heating sections is due to sensible heat. The effects of changes in diameter, heating wall temperature and charge ratio on the heat transfer performance of the looped PHP are also investigated and the results are summarized in Table II for both the unlooped and looped PHPs. Increasing the tube diameter and heating wall temperature increases the total heat transfer similar to that of the

Type of PHP	Th (C)	Surface tension	D (mm)	Charge ratio	Evaporative heat (W)	Sensible heat (W)	Percentage of sensible heat
Unlooped	120	σ	1.5	68.4%	1.44	30.49	95.5%
	120	3σ	1.5	68.4%	1.69	32.2	95%
	100	σ	1.5	68.4%	1.06	21.18	95.23%
	120	σ	3	68.4%	3.49	115.2	97%
	120	σ	1.5	89.5%	0	0	0
Looped	120	σ	1.5	64.21%	1.44	27.7	95%
	120	3σ	1.5	64.21%	1.6	30.18	94.9%
	100	σ	1.5	64.21%	1.1	17.8	94.1%
	120	σ	3	64.21%	3.28	109.16	97.1%
	120	σ	1.5	89.5%	0	0	0

Table II.
Effect of parameters on the performance of the PHPs

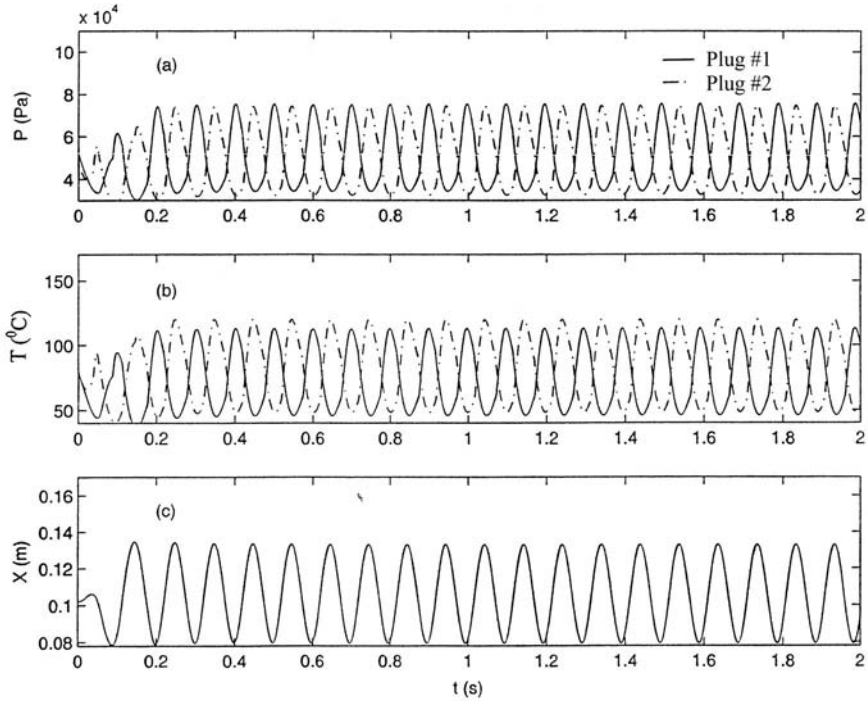

Figure 19.
Variation of pressure, temperature and the end positions with time for looped PHP

unlooped PHP. It can also be observed that increasing the charge ratio up to 90 per cent will stop the performance of looped PHPs. Calculated results show no circulation in the system, which is consistent with observations of Lee *et al.* (1999) and Miyazaki and Arikawa (1999).

6. Conclusions

Thermal modeling of both unlooped and looped PHPs with multiple vapor plugs and liquid slugs is proposed, and the behaviors of liquid and vapor plugs in the PHP are investigated. The following conclusions were obtained:

(1) For both unlooped and looped PHPs, periodic oscillation is obtained under specified parameters.

(2) Heat transfer in both looped and unlooped PHPs is due mainly to the exchange of sensible heat.

(3) Higher surface tension results in a slight increase in total heat transfer.

(4) For both unlooped and looped PHP, the total average heat transfer increased with increasing diameter.

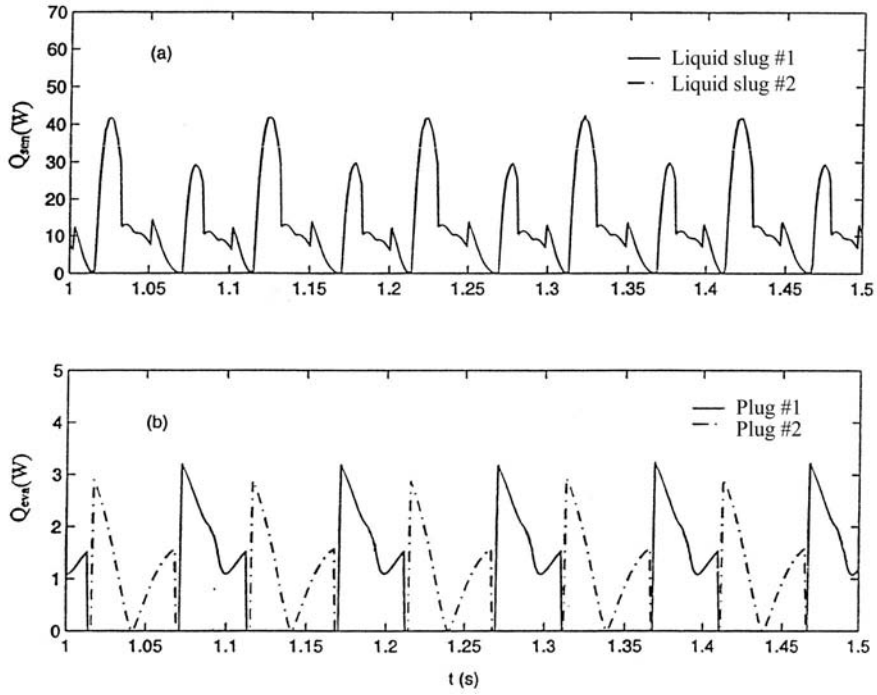

Figure 20.
Heat transfer rate; (a) sensible heat; (b) evaporative heat

(5) The total average heat transfer significantly decreased with a reduction in the heating wall temperature.

(6) The results show that both unlooped and looped PHPs could not operate for high charge ratios.

References

Akachi, H., 1994, Looped Capillary Heat Pipe, Japanese Patent, No. Hei6-97147.

Bejan, B. (1995), *Convection Heat Transfer*, 2nd edition, John Wiley & Sons, Inc, New York.

Dobson, R.T. and Harms (1999), "Lumped Parameter Analysis of Closed and Open Oscillatory Heat Pipes", *Proceedings of the 11th International Heat Pipe Conference*, Tokyo, Japan pp. 137-42.

Faghri, A. (1995), *Heat Pipe Science and Technology*, Taylor & Francis, Washington, DC.

Faghri, A. (1999), "Recent Advances and Challenges in Micro/Miniature Heat Pipes", *Proceedings of the 11th International Heat Pipe Conference*, Sep, 12th 1999, Tokyo, Japan.

Gi, K., Sato, F. and Maezawa, S. (1999), "Flow Visualization Experiment on Oscillating Heat Pipe", *Proceedings of the 11th International Heat Pipe Conference*, Tokyo, Japan pp. 149-53.

Hosoda, M., Nishio, S. and Shirakashi, R. (1999), "Meandering Closed-Loop Heat-Transport Tube (Propagation Phenomena of Vapor Plug)", in, *Proceedings of the 5th ASME/JSME Joint Thermal Engineering Conference*, March 15-19, San Diego, CA.

Kiseev, V.M. and Zolkin, K.A. (1999), "The Influence of Acceleration on the Performance of Oscillating Heat Pipe", *Proceedings of the 11th International Heat Pipe Conference*, Tokyo, Japan pp. 154-8.

Lee, W.H., Jung, H.S., Kim, J.H. and Kim, J.S. (1999), "Flow Visualization of Oscillating Capillary Tube Heat Pipe", *Proceedings of the 11th International Heat Pipe Conference*, Tokyo, Japan pp. 131-6.

Patankar, S.V. (1980), *Numerical Heat Transfer and Fluid Flow*, McGraw-Hill, New York.

Shafii, M.B., Faghri, A. and Zhang, Y. (2001), "Thermal Modeling of Unlooped and Looped Pulsating Heat Pipes", *ASME J. Heat Transfer*, Vol. 123, pp. 1159-72.

Wong, T.N., Tong, B.Y., Lim, S.M. and Ooi, K.T. (1999), "Theoretical Modeling of Pulsating Heat Pipe", *Proceedings of the 11th International Heat Pipe Conference*, Tokyo, Japan pp. 159-63.

Zhang, Y. and Faghri, A. (2002), "Heat Transfer in a Pulsating Heat Pipe With Open End", *International Journal of Heat and Mass Transfer*, Vol. 45, pp. 755-64.

Zhang, Y., Faghri, A. and Shafii, M.B. (2001), "Capillary Blocking in Forced Convective Condensation in Horizontal Miniature Channels, ASME", *J. Heat Transfer*, Vol. 123, pp. 501-11.